THERMAL PERFORMANCE ANALYSIS OF INDUCTION MOTOR

Omar Badran , Hussain Sarhan , Bilal Alomour

Al-Balqa` Applied University
Faculty of Engineering Technology
P.O.Box 331006, Amman 11134-Jordan

ABSTRACT

The aim of this paper is to apply a mathematical model using a lumped parameter thermal method and to conduct experiment test to determine the temperature distribution inside the induction motor to evaluate the thermal stability of the induction motor and to check whether the insulation of the copper windings is sufficient at different operating conditions, and to find out the hottest element which has the main effect on the operation and performance of the motor. We found out from the thermal model analysis that the hottest element in the induction motor is the end winding and rotor bars, this is due to stator copper losses and rotor bars losses which depend on the stator current, the stator current can be increased by increasing the torque or by decreasing the stator frequency, which makes the temperature of each element to increase. The thermal model of the induction motor is validated by comparing the calculated temperatures of each element in the induction motor with the experimental results that obtained from through thermocouples connected to the computer via data logger, and the results showed that the accuracy of the proposed thermal model has uncertainities of about 4% ~ 6% .

1. INTRODUCTION

IT IS extremely important to model the heat transfer behavior in the induction motor properly, as it defines the cooling capability, and consequently the nominal power of the machine. Accurate modeling of heat transfer is practically difficult without the finite element analysis (FE) due to the complex three dimensional geometries. Despite the fact that faster microprocessors are available, 3D FE analysis is yet time consuming (for dynamic thermal analysis), whereas different types of analytical methods can be applied easily to model the heat transfer in the machine instead [1-2].

Majority of the industrial electrical machines run continuously where the steady-state temperature is reached. Such applications are for example power plant generators, different kinds of conveyors, air conditioning motors, propulsion motors, etc. This has led to the fact that very often the heat transfer in electric machines is studied in the steady-state, and the heat capacitances of the machine are neglected in the model. Such a model is adequate enough for properly estimating the steady-state temperature rise of the machine; however, it cannot model the heat transfer mechanisms during the loading variations, [1-3].

High over loadings mean high losses, and consequently the temperature gradients are high. Therefore, in the present study the analytical heat transfer model for the motor is built, and the main interest is focused on the transient heat transfer mechanism during the loading variations. The model should be

flexible and computationally fast, and to be able to calculate the temperatures accurately, [1].

This study focuses on the thermal analysis of a three phase induction motor. During the operation of the induction motor, the heat generated losses (i.e. iron losses, stator copper losses and rotor losses) affects the efficiency and performance of the induction motor, where these losses can increase the temperature to a limit larger than the allowable operating temperature, which causes some important problems such as[4- 8]:

a) Thermal stresses which may exist in the rotor end rings and bars where most probably a motor breaks down.
b) Rising the resistance of the winding, and consequently rising the I2R losses.
c) Rising the temperature of stator winding insulation, and consequently the turn-to-turn or turn-to ground short-circuit may occur.
d) Increasing the temperature rise which has a direct effect on its useful service life. The higher temperature rise the shorter its useful service life.

The present thermal performance analysis can give a clear picture about the temperature distribution inside the induction motor that can accurately predict the hottest element which has the main effect on the induction motor performance.. Also the thermal model has been verified by the experimental work.

2.LITERATURE SURVEY

Most of the earlier researchers and designers have traditionally adopted thermal network model for on lumped parameter thermal model for electric machines both under steady and transient thermal conditions. (Lee, 2000) presented a thermal network method (TNM) to analyze thermal field of the induction motor which has air ducts in stator and rotor core as forced cooling channels. (Durán,

prediction of temperatures. This method predicted average temperatures quite accurately. (Rosenberryn, 1955) used thermal resistant networks to predict transient stalled temperatures of cast aluminum squirrel cage motors as early as 1955. (Mellor et al, 1991) have presented exhaustive study

2004) used the lumped-parameter thermal model for induction machines. His model considered just stator, rotor, and environment representative temperatures also parameter estimation has been carried out. (Okoro, 2005) used the lumped-parameter thermal model to predict both the steady-state and transient solution to the temperatures within a 7.5-kW induction machine.

A finite difference is one of the popular numerical methods widely used. Even though this method predicts hot spot temperatures, the method is not as flexible as finite element method in handling complex boundary conditions and geometry. (Williamson and Walker, 1991) used two dimensional times stepping finite difference scheme to solve the thermal transient problem. Pure analytical work is limited and it has too many major assumptions. While (Sreehivasan and Sengupta, 1977) used a one dimensional lumped model for predicting cooling curves in electric motors. They have determined the heat transfer coefficients on the surface as well as within the machine. However, the internal heat transfer coefficients used by them seems to be unrealistic. (Dokopoulos and Xypteras, 1982) predicted both rotor and stator winding temperatures analytically. However, they assumed that the model is made of rings placed one over another with constant lengths. (Witzak, 1986) solved analytically the two dimensional model containing only one slot pitch of the stator. He assumed that there is no heat interaction between rotor and stator.

The use of finite elements method for thermal analysis of induction motor has wide acceptance among researchers in recent years. (Gnffith and Mc Coy, 1986) used ANSYS package for three dimensional analysis of electromagnetic and thermal behavior of induction motor rotors. (Liu, 2000) used the finite element method to solve the three-dimensional steady-state and/or transient heat flow equation which described the thermal model of the induction motor. (Siyambalapitiya et a1, 1988) studied the failures of large cage rotors of induction motors using three dimensional finite element electrical- thermal analysis of bar and end rings. (Rajagopal et al, 1994) carried out two dimensional steady state thermal analyses of electric machines using FEM.

3.ELECTROMAGNETIC MODEL

3.1 Equivalent Circuit

The analysis of the 3-phase induction motor is simplified by means of per- phase equivalent circuits. The per-phase equivalent circuit is shown in Fig.1, and it is similar to the equivalent circuit of a transformer. The inputs for the electromagnetic motor model are the frequency, the voltage, and the torque, and the model outputs (currents and voltages), the electromagnetic torque, and the slip. From the currents and the voltages, the different loss components of the machine are calculated in a loss calculation block connected between the electromagnetic and thermal parts of the model [2-3, 9].

The losses as a function of motor parameters slip(s) and applied stator voltage (v), requires analysis of the complete

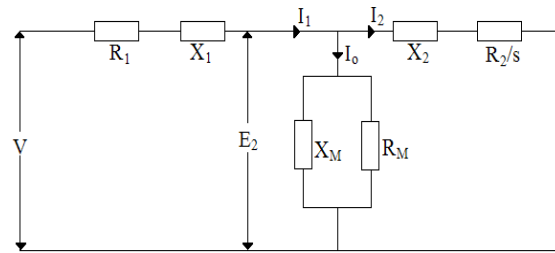equivalent circuit model of an induction motor, including both rotor and stator as shown in the Figure 1.

Figure 1- Equivalent circuit of induction motor, [3].

The stator circuit includes stator resistance R1, stator leakage reactance X1, resistance RM , which accounts for hysteresis and eddy-current losses in the iron, and magnetizing reactance XM, which accounts for the magnetizing component of the exciting current. The rotor circuit includes rotor resistance R2, and rotor leakage reactance X2. From Fig.1 there are three currents in the circuit, stator current I1 , rotor current I2 , and exciting current I0 they are divided in two parts, magnetizing component of exciting current , and core loss component of exciting current .

Induction motor losses may be readily determined by first solving the equivalent circuit shown in the Figure 1 for I1, I2, and E2 and then substituting into the appropriate equations to calculate the motor losses [2-3,9].In order to find the stator current, we should determine the stator impedance Z1 , the rotor impedance Z2 , and the magnetizing impedance Z0 .

The stator impedance is obtained from the following equation:

$$Z_1 = R_1 + jX_1 \qquad (1)$$

The rotor impedance is obtained from the following equation:

$$Z_2 = \frac{R_2}{s} + jX_2 \qquad (2)$$

The magnetizing impedance is obtained also from the following equation:

$$Z_0 = \frac{R_m * jX_m}{R_m + jX_m} \qquad (3)$$

Then the value of the Zp which represents the equivalent impedance of the rotor impedance Z2 and magnetizing impedance Z0 can be found from the following equation:

$$Z_p = \frac{Z_2 * Z_0}{Z_2 + Z_0} \qquad (4)$$

Finally, the total equivalent impedance of the stator impedance Z1, and the rotor impedance Z2 and magnetizing impedance Z0 is given by:

$$Z_{in} = Z_1 + Z_p \qquad (5)$$

Then, the magnitude of stator current is determined from the following equation by applying the ohm's law in the circuit shown in Figure 2:
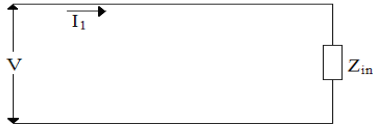
$$I_1 = \frac{V}{Z_{in}} \tag{6}$$

Figure 2 - Equivalent circuit of induction motor with total impedance.

The induced voltage in the rotor E2 can also be found form the following equation:

$$E_2 = I_1 Z_p \tag{7}$$

Then the rotor current I2, can be found from applying the ohm's law on the rotor circuit as shown in Figure 2, [2, 3, 9]:

$$I_2 = \frac{E_2}{Z_2} \tag{8}$$

3.2 Heat losses calculation

When the induction motor is used to drive the load connected on its shaft, it encounters losses, which serve as heat sources distributed throughout the whole induction motor and vary with different operating conditions. The power losses of induction motor consist of three main factors as shown in flow chart in Figure 3.
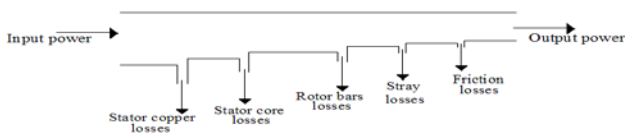

Figure 3- Flow chart of the heat losses in the induction motor, [2- 4, 9-10].

power	1.5 kW
Rotor speed	2840 r/min/3405 r/min
Phase number	3
Voltage	220-380/240-420 V
Current	5.9-3.4/5.4-3.08 A
frequency	50 Hz / 60 Hz

Table 1. The Characteristic Information Of The Used Induction Motor

The three main parts included in the flow chart and shown in Figure 3, [2-3,9], are:

a) Stator Copper losses: these losses are produced when the Current passing through the stator windings, and generates the heat and consequently, the temperature of the motor rises. These losses are dependent on the square of stator current and they are calculated from the following equation :

$$P_{scl} = 3I_1^2 R_1 \tag{9}$$

b) Rotor bars losses: these losses are produced when the current passing through the rotor bars, they are dependent on the square of rotor current, and they are calculated from the following equation:

$$P_{rol} = 3I_2^2 R_2 \tag{10}$$

c) Iron losses: Iron losses are generated in the conducting core laminations, due to hysteresis, eddy-current. The core losses can be calculated from the following equation:

$$P_{core} = 3\left(\frac{E_2^2}{R_m}\right) \tag{11}$$

3.3 Induction Motor Tests

(No-Load Test, Blocked Rotor Test)

We used an 1.5 KW three phase induction motor to make our analysis, therefore the equivalent circuit parameters must be known, and the equivalent circuit parameters for an induction motor can be determined using specific tests on the induction motor such as: DC test to determine the value of R2 , Blocked Rotor Test which used to determine the values of X1, X2, and R2, and No-Load. Test which used to determine the magnetizing reactance XM [2-3,9,11-12] .

The induction motor used in the study is three phase squirrel cage rotor induction motor of type (Y 90S-2). Table 1 shows the information related to the used induction motor

Y series three-phase induction motors are totally-enclosed fan cooled squirrel-cage AC asynchronous motors , it has a lot of advantages including high efficiency , energy saving , large starting torque ,excellent performance , low noise , low vibration, high reliability , and convenient operation and maintenance. Also the Y series induction motors are fit for the common applications like: metal cutting machines, pumps, blowers, transportation machineries, puddle mixers, agricultural machineries, and foodstuff processing machineries.

Figure 4- The used induction motor.

The equivalent circuit parameters (stator resistance, rotor resistance, stator reactance, rotor reactance and magnetizing reactance) which are obtained from the tests applied to the induction motor is shown in the Table.2.

Parameter	Value (Ω)
R_1	4.1667
R_2	3.33
X_1	4.72
X_2	7.08
X_M	111.3

Table 2. Equivalent Circuit Parameters Of Induction Motor

These parameters are fed to the Matlab simulation of the induction motor, to be used for calculating the induction motor power losses (stator copper losses, rotor bar losses and stator core losses).

3.4 Variable-Frequency Induction Motor Drive

The induction motor requires a variable-frequency drive for variable-speed operation. The drive circuit consists of three main components, a SCR rectifier connected to an inverter through a DC link. Figure 5 shows a block diagram of the power circuit of a typical variable-frequency induction motor drive.
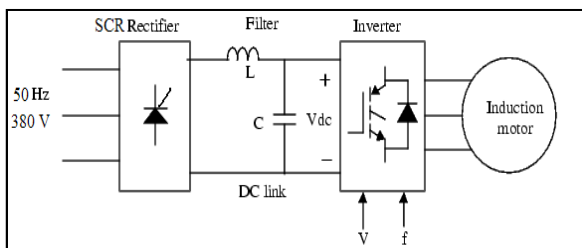

Figure 5- Block diagram of the variable frequency induction motor drive.

The rectifier circuit designed from thyristors which covert AC supply voltage to DC voltage, where the supply voltage can be controlled at different values by inserting a proper firing angle to the SCR rectifier circuit, and then the DC voltage signal is filtered from noises via a certain capacitor before going to the IGBT inverter. The inverter consists essentially of six power switches which are made of

insulated gate bipolar transistors (IGBT); the IGBT inverter converts the DC link voltage into an adjustable three-phase AC voltage. Different control schemes can be used to control the inverter output voltage and frequency. One of the most utilized schemes is pulse width modulation (PWM) to obtain three-phase variable sinusoidal voltage waveforms by modulating the on and off.

The inverter control circuit is implemented using Matlab simulink as shown in Figure 6. In this model the volts/Hertz is kept constant, so that when we change the frequency, the voltage is changed linearly using SCR rectifier by choosing a proper firing angle in order to keep V/f constant.

When we change the value of the stator frequency to a small value (25 Hz, 15 Hz), we must change the value of the voltage to the value that keeps the V/fs ratio constant, in order to keep the motor flux in the air gap to be constant, to avoid over heating of the induction motor to a limit that not exceeds the temperature size and damage the insulation, therefore in order to maintain the motor flux, the (V/fs) has to be kept constant as shown in the equation below [2]:

$$(V / F_s) = 4.44 N_1 \phi_m \qquad (12)$$

Where: N1: the number of coils in the stator. ϕ_m : The motor flux

Figure 6- Matlab simulation of inverter control of the induction motor.

4. THERMAL MODEL OF THE INDUCTION MOTOR

4.1 thermal network model

The lumped-parameter thermal method has been used for a very long time by several researchers, [4-5,8,13] to predict temperature rise at different parts of the induction machine, therefore we have used this method to make a thermal analysis of the induction motor in the present research, for totally-enclosed induction motors using lumped parameter

thermal method. Kessler (1960), Mellor et al,(1991) and Kylander (1995) used lumped parameter thermal method and assumed that the temperature of the solid is spatially uniform at any instant during the transient process, this assumption implies that temperature gradient within the solid are negligible. In developing the The lumped method assumed that the induction motor geometry should be divided into basic elements due to their different losses, and therefore different temperature rises as shown in the Figure 7, for example the stator winding is divided into two elements(the slot winding and end winding).

Therefore, each element is assumed to be identified by a node in the thermal model with its corresponding thermal capacitance and heat source. The choice of subdividing the induction motor into elementary components remains a compromise between the simplicity of the model and the accuracy required of the results [4-5]. It has been shown by Kylander (1995) that high level of accuracy could be achieved by subdivision of the induction motors geometrical parts. The thermal model of the induction motor is shown in Figure 8. The model consists of 10 nodes and 14 thermal resistances. In the model, the stator of the induction motor has networks for the stator iron, stator winding, and the end windings. It is assumed that the heat transfer from the rotor winding through the air gap goes directly to the stator winding with negligible impact on the stator teeth. By connecting the networks for the rotor, stator and frame together through thermal resistances, the thermal network model for the induction motor is realised.

Individual components which are comprised in the thermal model, is shown in Figure 7, are:

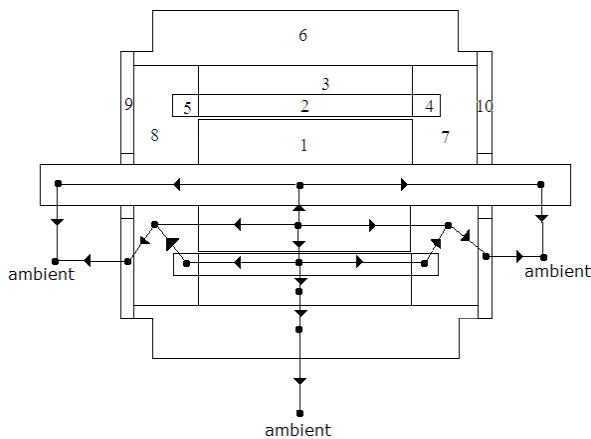|	
1. Rotor bars	2. Slot stator winding
3. Stator core	4. Right end winding
5. Left end winding	6. Round frame
7. Right end-cap air	8. Left end-cap air
9. Left side frame	10. Right side frame

Figure 7- Longitudinal cross section of induction motor, showing the main elements of the present thermal model.

Thermal model of the induction motor is build based on the main directions of the heat flows in the induction motor as shown in Figure 7, these directions of heat flow can be summarized as:
1. There is a heat flow from the rotor bars through the air gap towards the stator winding and then to the stator iron

then finally to the ambient through the round frame by convection.

2. There is a heat flow from the stator end-winding and the rotor bars sides towards the end-cap air by convection and then to the ambient through the side frame by convection.

The thermal model of the induction motor is shown in figure 8 and contains the following components:

1. Heat sources : which are generated in the motor due to the losses , these losses includes:

   a) Stator copper losses Pscl :(which are generated in the stator winding, node 2, and end winding, nodes (4, 5), and due to supply currents).
   b) Stator core losses Pcore :(which are generated in the stator core, node 3, due to eddy currents and hysteresis).
   c) Rotor bar loss Prol :(which are generated in the rotor bars, node 1, due to induced currents in the bars).

2. Thermal resistance: connect between each two neighboring nodes, this thermal resistance impedes the heat transfer from one component through the other, it depends on the geometric and properties of the material.

3. Heat capacitances: measures the ability of each element to store energy with time, and it depends on the some properties of the material such as: specific heat and density.
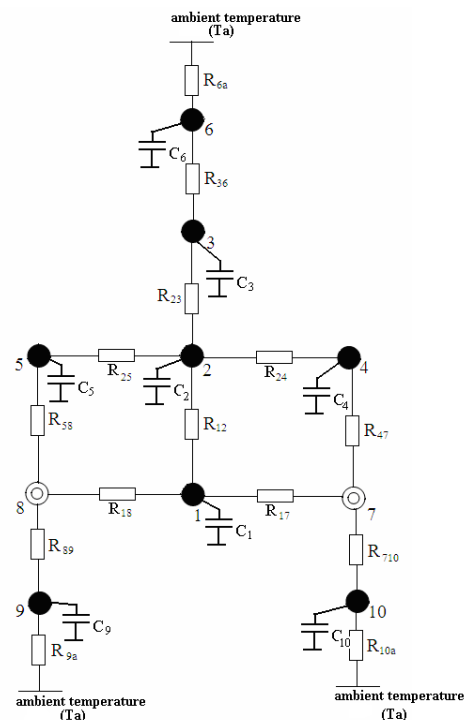

Figure 8- thermal model of induction motor.

4.2 Mathematical analysis

Mathematical equations that describe the thermal behavior of the induction motor are usually derived from the basic

energy balance equations that follow the general form such as;

$$\begin{pmatrix} \text{rate of energy} \\ \text{stored} \\ \text{within system} \end{pmatrix} = \begin{pmatrix} \text{heat flow} \\ \text{rate} \\ \text{into system} \end{pmatrix} - \begin{pmatrix} \text{heat flow} \\ \text{rate out of} \\ \text{system} \end{pmatrix} + \begin{pmatrix} \text{rate of heat} \\ \text{generated} \\ \text{within system} \end{pmatrix} \quad (13)$$

For a stationary system composed of a material of density ρ, specific heat Cp, and constant volume V, the balance equation takes the form:

$$\rho C_p V \frac{dT}{dt} = Q_{in} - Q_{out} + Q_{gen} \quad (14)$$

Equation (14) can only be used if there is a temperature distribution in the system, or a part of the system is uniform, the assumption about the uniformity of the temperature distribution implies that the system physical properties, such as density and specific heat, are constant within the system boundaries [10,14-16].

4.2.1 Heat transfer methods

Power dissipation in an electrical component will lead to a complex process of combined heat conduction, convection and radiation. Heat conduction takes place only through molecular communication, while the convective heat transfer takes place in moving liquid or gas. Thermal radiation is electromagnetic radiation that the body emits based only on its temperature. However, in practice a simplified thermal conduction and convection model is often defined in the thermal model of electrical devices. In this section the description of the basic heat transfer concepts will be discussed. In general, there are three mechanisms to dissipate the heat energy due to losses in the induction motor; convection, conduction, and radiation [14-16].

a)   Conduction heat transfer

Conduction is the mechanism that transfers the heat inside the solid medium, in thermal modeling, heat flux Qth can be calculated from the following equation [20]:

$$Q_{th} = KA \frac{\Delta T}{\Delta x} \quad (15)$$

And by introducing the thermal resistance Rth due to conduction:

$$R_{th} = \frac{\Delta T}{Q_{th}} = \frac{\Delta x}{KA} \quad (16)$$

Heat transfer can thus be modeled in a manner that is analogous to Ohm's law.

b)   Convection heat transfer

Heat energy transfers between a solid and a fluid when there is a temperature difference between the fluid and the solid. This is known as convection heat transfer. Generally, convection heat transfer cannot be ignored when there is a significant fluid motion around the solid. The fluid acts as a temporary heat sink. The physical body shapes of the components or devices as well as the surrounding fluid characteristics define the heat convection properties.

By convection, heat is transferred from solid to either gas or liquid through the surface layer, always from the higher temperature to the lower. Convection can be either natural or forced convection, depending on whether there is an external device, such as a fan or a pump, which forces the gas or cooling liquid to flow. In natural convection, heat transfer is caused by the gravity acting on the density variations near the boundary section of the two medium. Dissipated power due to convection can be expressed as, [14-16]:

$$Q = hA(T_s - T_\infty) \quad (17)$$

Where A is the area, Ts is the temperature, and the coefficient h is the convection heat transfer coefficient. The value for the thermal resistance used in the calculations that describes the convective heat transfer across the surface, can be calculated as:

$$R_{th, conv} = \frac{1}{Ah} \quad (18)$$

c)   Radiation heat transfer

Heat flux dissipated by radiation can be expressed with Stefan-Boltzmann's equation:

$$Q_{th} = \in \sigma_{SB}(T_1^4 - T_2^4) \quad (19)$$

Where ε is the emissivity, σSB Stefan-Boltzmann's constant (5.67×10-8 J/s/m2/K4), and T the temperature. Emissivity ε varies from 0 of "transparent" material to 1 of a black body. In this analysis, radiation is neglected, because the temperature of the induction motor is not enough high to radiate the heat, [15].

4.3 Differential equations of the thermal model:

By applying the basic energy balance (Equation 14), on each node in the thermal model of induction motor Figure 8, the differential equations can be formulated to describe the thermal behavior of induction motor in steady and transient states at certain operating conditions. We have considered each node as a lumped system, which has a control volume like a boundary that defines the heat enters the system or leaves it, and the generated heat within the system. We assume that the temperature is distributed uniformly in each part of the induction motor; this assumption is similar to Frank and David, 2002 model. The linear deferential equations of the thermal model of the induction motor (equations, 20 to 29) can be rewritten in a matrix form as a state space representation form as shown in Figure 9.

Figure 9- State space representation equation for the induction motor

Parameters	Value	Parameters	value
power	1.5 KW	Stator inductances	4.72 Ω
Rotor speed	2840 r/min/3405 r/min	Magnetizing inductance	111.3 Ω
Phase number	3	Rotor inductance	7.08 Ω
Voltage	220-380/240-420 V		
Current	5.9-3.4/5.4-3.08 A		
frequency	50 Hz / 60 Hz		
Stator resistance	4.167 Ω		
Magnetizing resistance	1187.48 Ω		
Rotor resistance	3.333 Ω		
Slot number	18	Stator length	82 mm
Stator diameter	131.5 mm	Rotor length	82 mm
Housing diameter	145 mm	Motor length	208.5 mm
Stator bore	72.5 mm	End winding extension	50 mm
Tooth width	5 mm	End winding inner diameter	72.5 mm
Slot depth	16 mm	End winding outer diameter	104.5mm
Air gap	0.5 mm	Bearing diameter	52 mm
Rotor diameter	71.5 mm	Bearing width	15 mm
Shaft diameter	29.5 mm		

Table 3. Dimensions and the specifications of the three phase induction motor typ

In order to calculate the temperatures of each element in the induction motor, we must know firstly, the values of the losses in the induction motor; therefore electromagnetic model is needed to find them. Then we must find the thermal resistances and capacitance of each element in the induction motor, they depends on the system physical properties, such as: density and specific heat and, thermal conductivity as shown in Table.4. They depend also on the geometrical dimensions of the induction motor as shown in Table.3.

$$C_1\frac{dT_1}{dt} = P_{rol} - (G_{12} + G_{17} + G_{18})T_1 + G_{12}T_2 + G_{17}T_7 + G_{18}T_8 \quad (20)$$

$$C_2\frac{dT_2}{dt} = P_{scl,sw} - (G_{23} + G_{24} + G_{25})T_2 + G_{23}T_3 + G_{24}T_4 + G_{25}T_5 \quad (21)$$

$$C_3\frac{dT_3}{dt} = P_{core} - (G_{23} + G_{36})T_3 + G_{23}T_2 + G_{36}T_6 \quad (22)$$

$$C_4\frac{dT_4}{dt} = P_{scl,ew} - (G_{24} + G_{47})T_4 + G_{24}T_2 + G_{47}T_7 \quad (23)$$

$$C_5\frac{dT_5}{dt} = P_{scl,ew} - (G_{25} + G_{58})T_5 + G_{25}T_2 + G_{58}T_8 \quad (24)$$

$$C_6\frac{dT_6}{dt} = P_{r-frame} - (G_{36} + G_{6a})T_6 + G_{36}T_3 + G_{6a}T_a \quad (25)$$

$$C_7\frac{dT_7}{dt} = P_{capair} - (G_{47} + G_{17} + G_{710})T_7 + G_{47}T_4 + G_{17}T_1 + G_{710}T_{10} \quad (26)$$

$$C_8\frac{dT_8}{dt} = P_{capair} - (G_{58} + G_{18} + G_{89})T_8 + G_{58}T_5 + G_{18}T_1 + G_{89}T_9 \quad (27)$$

$$C_9\frac{dT_9}{dt} = P_{s-frame} - (G_{89} + G_{9a})T_9 + G_{89}T_8 + G_{9a}T_a \quad (28)$$

$$C_{10}\frac{dT_{10}}{dt} = P_{s-frame} - (G_{710} + G_{10a})T_{10} + G_{710}T_7 + G_{10a}T_a \quad (29)$$

Material	Thermal conductivity (W/m.C)	Density (Kg/m^3)	Specific heat (J/Kg.C)
Iron	58	7850	420
Aluminum	222	2790	833
Steel	35	7770	460
copper	388	8933	385
Ambientair	0.02624	1.127	1007

Table 4. The physical properties of the materials in induction motor.

5. MATLAB SIMULATION OF ELECTROMAGNETIC MODEL

After the determination of induction motor parameters (stator and rotor resistances and reactances) from the induction motor tests (DC test , No load test ,and Blocked rotor test) as shown in Table.2 , these parameters are inserted as an inputs to Matlab simulation (Induction Motor model) and shown in the Figure 6, in order to find the induction motor characteristics like stator current ,rotor current ,and the rotor speed which are fed to the power losses block shown in Figure 6, in order to determine the power losses (the stator copper losses (Pscl), rotor bar losses (Prol), and stator core losses (Pcore)) , with the variations of the applied torque at different values of the stator frequency (50 Hz, 25 Hz, and 15 Hz) .

The values of the power losses (stator copper losses (Pscl),rotor bar losses (Prol),and the stator core losses(Pcore))

of the induction motor are dependent on the value of the stator current (I1). When the stator current increase the power losses increases and vice versa.

We have noticed that the stator copper losses and rotor bars losses Figure 10 and Figure 11 are increased with the increasing the applied torque, because the rotor speed decrease leading the slip to increase and eventually the stator current increase which leads the stator copper and the rotor bars losses to be increased according to the equations (10 and 11). These power losses results found to be dependent on the stator current, I1, and the rotor current, I2 the latter is depends on the stator current value. Therefore the stator copper losses are proportional to the square of the stator current and the rotor bars losses are also proportional to the square of the rotor current. So that, when the stator current increases the power losses will increase, as shown in the Figures, 10 and 11.

6. EXPERIMENTAL TEST FOR THE INDUCTION MOTOR

The experimental setup used for the thermal modeling validation is presented in Figure 12; it shows the main parts of the setup, where: (a) JLEM three phase 1.5 kW induction motor (b) thermocouples (c) brake torque (d) data logger (e) inverter(f) Power source (g) torque measurement unit (h) electrical measurement units (k) computer.

Temperature measurements of the induction motor were carried out at rated load and at load variation, under different values of the stator frequencies (50 Hz, 15 Hz, and 25 Hz). Therefore, seven thermocouples Type K were installed in the stator core, end-windings and the frame of the induction motor as shown in Figure 12.
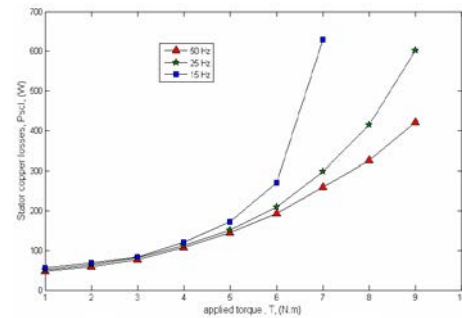

Figure 10- stator copper losses at different values of the applied torque and stator frequencies.
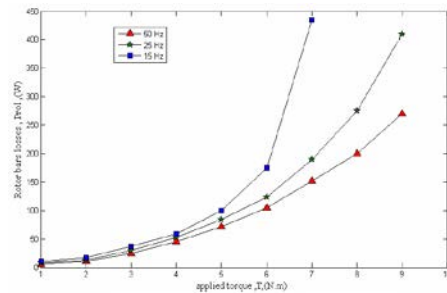

Figure 11- Rotor bars losses at different values of the applied torque and stator frequencies.

All the thermocouples were connected to a 15-channel programmable data logger for recording the temperature for each element, as shown in the Figure 12. Through the built-in RS232 interface the measured data stored in a computer hard disk and the software evaluates the measured data. The machine was allowed to run at rated load for two hours until thermal equilibrium was attained, and then repeated for the other values of the stator frequency.

The accuracy of the thermal model described in chapter three has been evaluated by comparing the results obtained numerically by the electromagnetic thermal model and those obtained by the experiment in the specified conditions.

It is important to add that only the temperatures of the stator parts were recorded since the rotor parts were inaccessible during motor operation.

The accuracy of the thermal model described in chapter three has been evaluated by comparing the results obtained numerically by the electromagnetic thermal model and those obtained by the experiment in the specified conditions.

The Matlab simulation of the thermal model has been built as shown in Figure 13, to find out the temperatures of each element in the induction motor. This Matlab simulation can determine the heat losses in the induction motor at the rated conditions from the structured induction motor model, and then these heat losses are inserted in the next step to the thermal model to find the temperature of each element in the induction motor at rated conditions, and at small values of the stator frequency.

Figure 12- experimental setup used for validating the thermal model of JLEM three phase 1.5 kW induction motor.

7. MATLAB SIMULATION OF THE THERMAL MODEL OF INDUCTION MOTOR

7.1 Determining the temperatures of each element in the induction motor by running it continuously at rated conditions at different values of the stator frequency:

Firstly, we have determined the temperature of each element in the induction motor by running it continuously at ambient temperature equal to 30 oC, at rated conditions (line to line voltage =380V, stator current=3.8A, stator frequency frequency=50Hz, rated load =5 N.m at, output power = 1500W, star connection, and 2poles), the induction motor parameters (stator and rotor resistances and reactances) are obtained from the tests which applied to the induction motor as listed in Table.2. The induction motor parameters are used to determine the heat losses (stator copper losses, rotor bars losses and the stator core losses) at rated conditions, and inserted to the thermal model to find the temperature of each element in the induction motor.

Secondly, we have run the induction motor at a small values of the stator frequencies such as (15 Hz, 25 Hz) at same rated load, in order to see the effect of the stator frequency changes on the induction motor elements temperature, we have taken in consideration the changes of the stator frequency according to the V/f ratio, which must be constant during the operation of the induction motor.

7.2 Determining the temperatures of each element in the induction motor by running it discretely at different values of torque and different values of stator frequency:

To study the effect of applying different values of torque on the induction motor at different values of stator frequency (15 Hz, 25 Hz, and, 50 Hz) according to the signals shown in the Fig.14. The value of the torque is changed while the induction motor is running at different interval periods of time, to see how the temperature of each element will behave under this kind of signals . From the Matlab simulation shown in the Figure 13, we have changed the value of the applied torque at different time intervals as shown in Figure 14; the induction motor ran at (50 Hz). Then we changed the value of the stator frequency to a small values (25 Hz and to 15 Hz) using the PWM, taking into account the value of the ratio V/f to be constant, therefore, the value of the firing angle is changed in order to obtain the desired supply voltage, to notice how the motor elements temperature changes.
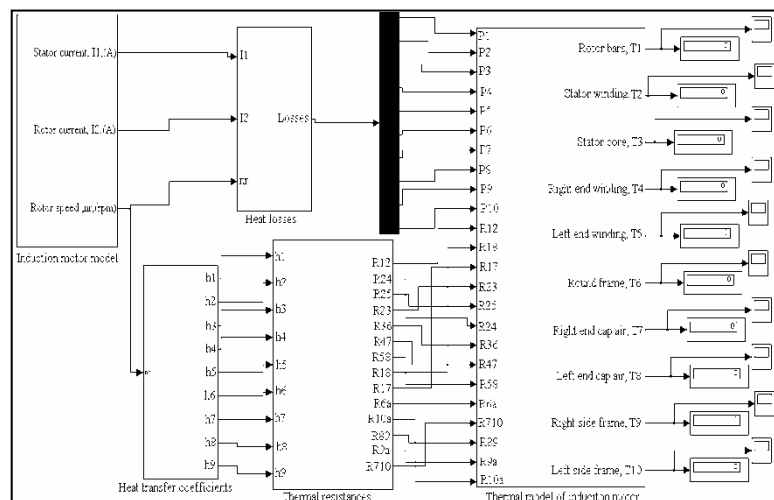

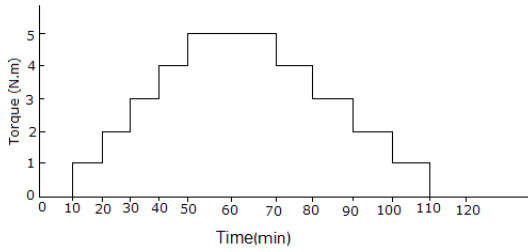Figure 13- Matlab simulation of thermal model of induction motor for determining the temperature distributi

Figure 14- The applied torque signal at different values.

8. THE RESULTS:

After running the thermal model for the induction motor continuously at rated load (1500 kW, 380V, 50Hz), to find out the temperature of each element in the induction motor, then we notice temperatures change with decreasing the value of the stator frequency (25 Hz, and 15 Hz) at the same rated load, these temperatures are plotted versus time as shown in Figure 15 to Figure 16. These temperatures from the mathematical model are compared with the experimental results at different values of the stator frequency.

We noted from the results of the simulation of thermal model that the hottest element in the induction motor is the stator end winding and the rotor bars as shown in the Figure 15,and Figure 18 , this could be due to the stator copper losses and the rotor bars losses; because they are dependent on the stator current which is considered the main factor in heating the induction motor . So that the stator current increased due to the increase of the applied torque .
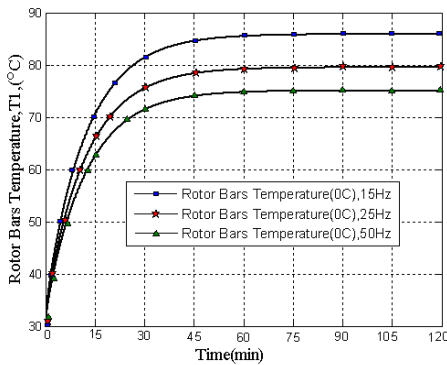
Figure15- Temperature of the Rotor bars at the rated load at different values of the stator frequency.
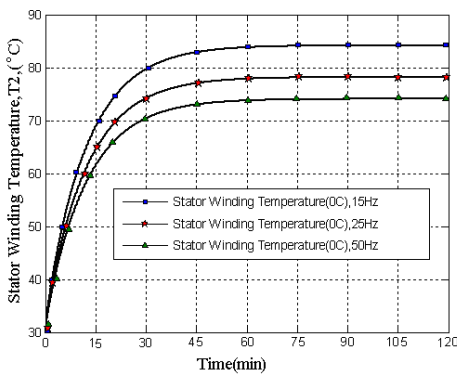
Figure16-Temperature of the stator winding at the rated load at different values of the stator frequency
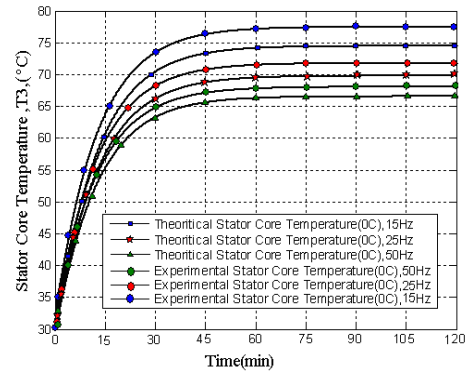
Figure 17- Temperature of the stator core at the rated load at different values of the stator frequency
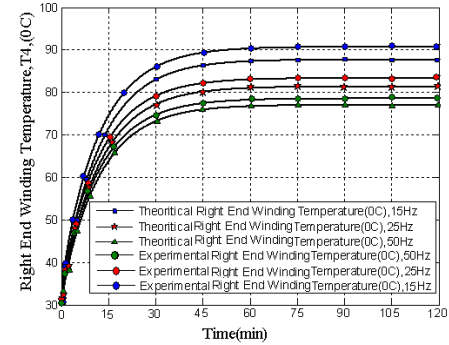

Figure 18- Temperature of the Right end winding at the rated load at different values of the stator frequency.
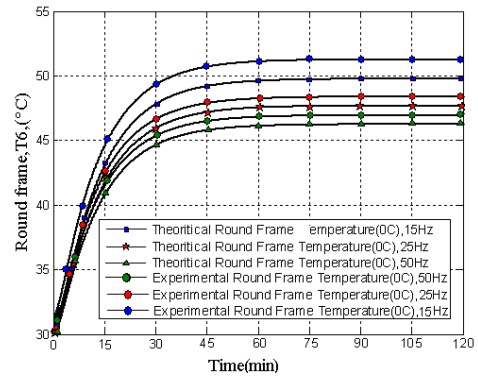

Figure 19- Temperature of the round frame at the rated load at different values of the stator frequency.
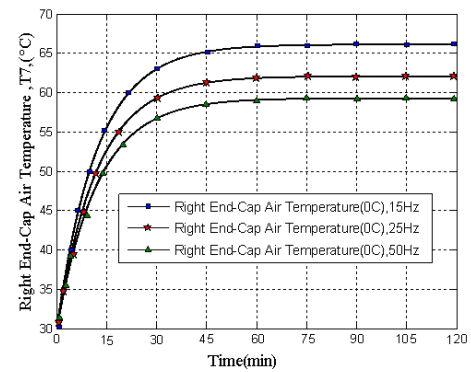

Figure 20- Temperature of the Right end cap air at the rated load at different values of the stator frequency.
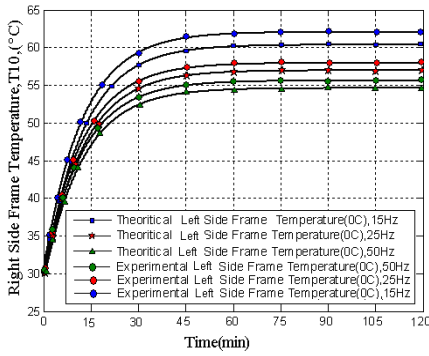
Figure 21- Temperature of the Right side frame at the rated load at different values of the stator frequency.

Reducing the stator frequency at constant load leads to the increase of stator copper and rotor bars losses which increase the heat of the induction motor, that will draw a higher stator current to compensate the reduction in the magnetic flux.

The temperature of the end winding element in the induction motor at rated load and at stator frequency of 50 Hz is 77 0C, which is less than the allowable temperature (120 0C), but when we have reduced the stator frequency to a smaller frequency values of 25 Hz, and 15 Hz and the same rated load , the induction motor draws larger stator current than the rated stator current , which means that the stator copper losses and the rotor copper losses will increase, pushing the induction motor elements temperature -specially the end winding – to increase more and more to the limit exceeds sometimes the allowable temperature level . This high temperature will damage the insulation of windings and burnout the induction motor, while the temperature of the end winding at 25 Hz is about 82 oC and at 15 Hz is about 90 oC, as shown in the Figure 18 . So, it is clear that the end winding temperature is larger than that at 50Hz, because the synchronous speed is reduced by reducing the stator frequency. At the same rated torque the induction motor will draw more stator current to compensate the leakage in the stator flux, as well as the heat transfer coefficients inside and outside the induction motor is decreased because the synchronous speed is reduced due to reducing the stator frequency, and this increase the values of the thermal resistances which allow the temperature of each element in the induction motor to be increased more and more.

The thermal model simulation for the induction motor at different torques and at different stator frequencies (50 Hz, 25 Hz, and 15 Hz) is tested . It is found that the temperature of each element in the induction motor has increased with decreasing the stator frequency. The results of temperatures are plotted versus time as shown in the Figures 22 to 27.

The results showed that the hottest temperature is also at the end winding and rotor bars elements, therefore from Figure 22, and Figure 26, the end winding temperature at 50 Hz and no load increased to 44 oC then increased to (47, 50, 57, 65, and 77 0C) at different applied torque (1, 2, 3, 4, and 5 (N.m)) respectively, we noted that the temperature is increased by increasing the applied torque the increase of the stator current. Then the applied torque is decreased from 5 N.m to (4, 3, 2, and 1 N.m) , so that the temperatures were

dropped to (67, 58, 53, and 490C) respectively. We have noticed that when the torque reduced from 5 N.m to 4 N.m, the temperature of the end winding is higher than 65 oC, and this due to the heat capacitance at the end winding that is responsible of storing heat in the end winding, therefore the end winding doesn't lose all the heat. Then the stator frequency again reduced to small values (25 Hz, and 15 Hz), we have noticed that the temperature of the end winding is increased to levels larger than those at 50 Hz as shown in Figure 26 for the right and left end winding, because the induction motor draws a larger stator current that is responsible for increasing the heat losses to a larger values that lead to a quick heating of the induction motor to levels may be larger than the allowable temperature level, which will speed up the damage the induction motor .

We have plotted the temperature of the stator end winding, rotor bars, and round frame versus the applied torques as in Figures 28 to 30, the temperature of the induction motor elements are changed with the applied torques and at different stator frequencies. The torque applied to the induction motor is in continuous form, until the induction motor elements temperatures reached to the steady state, then this process is repeated at other value of the applied torque and so on, finally we plot the temperature versus the applied torque is plotted.

To validate the present thermal model results of the induction motor, it's necessary to compare the results with the results of different thermal models done by other researchers [1], [2], and [3], to see the main differences of the temperature change between different studies. Different studies were mentioned here for comparison purposes as following:
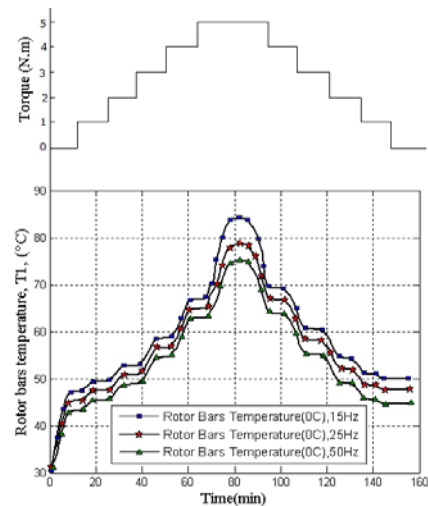

Figure 22- temperature of the Rotor bars at different values of the applied torque and at different values of the stator frequency.
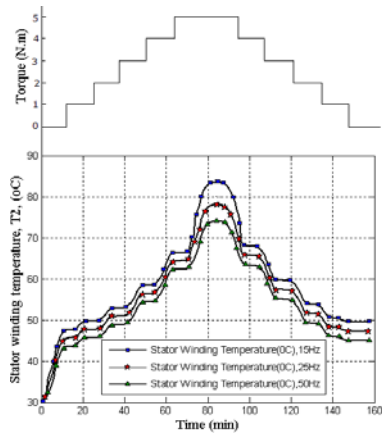
Figure 23- temperature of the Stator winding at different values of the applied torque and at different values of the stator frequency.
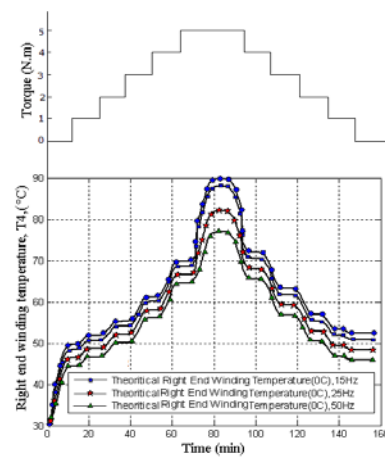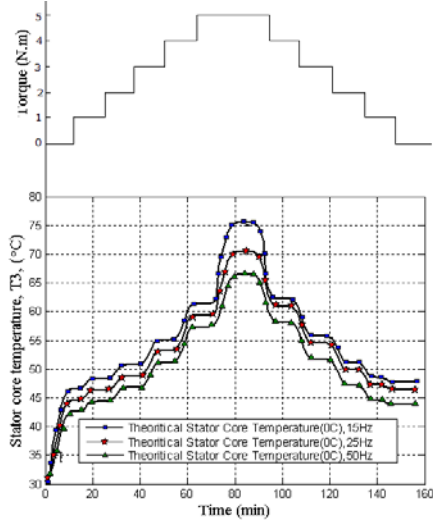

Figure 24- temperature of the stator core at different values of the applied torque and at different values of the stator frequency.
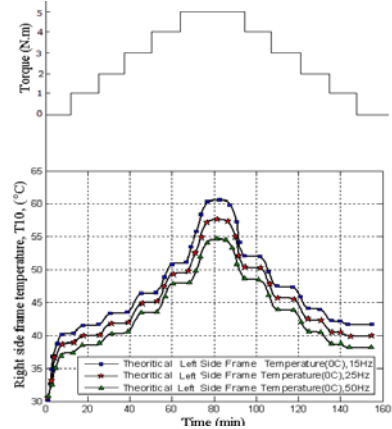

Figure 25- temperature of the Round frame at different values of the applied torque and at different values of the stator frequency.

Figure 26- temperature of the Right end winding at different values of the applied torque and at different values of the stator frequency.

Figure 27- temperature of the Right side frame at different values of the applied torque and at different values of the stator frequency
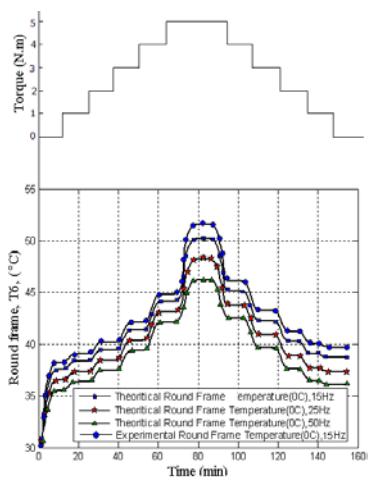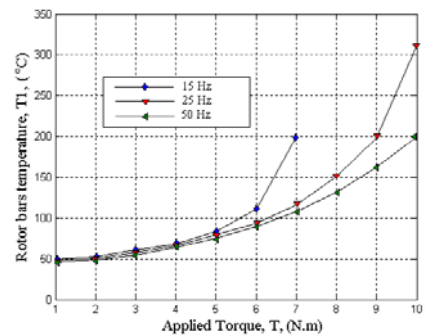

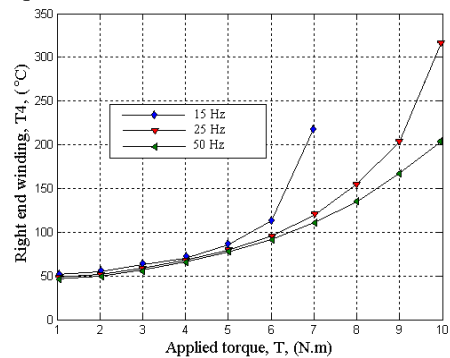Figure 28- the temperature of the rotor bars versus the applied torque.

Figure 29- the temperature of the End winding versus the applied torque
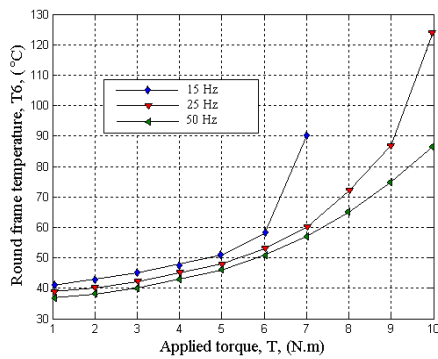
86

Figure 30- the temperature of the round frame versus the applied torque.

(Ogbonnaya, 2005) focused on the Steady and transient states thermal analysis of a 7.5-kW squirrel-cage induction machine at rated-load operation , therefore ,we found that the end winding temperature of Ogbonnaya thermal model is close in trend to our end winding temperature results. (Shenkman ,2005) determined the thermal behavior of induction motors under different synchronous speeds, his temperature curves trend is very close to our temperature curves, he found that when the synchronous speed is reduced, the temperature will increase at the same load, this is consistent with our results as well. (Al-Tayie, Acarnley, 1997) determined the temperatures of the stator and the rotor at a different torque values, their temperature curves trend is very close to the temperatures results of the our thermal model for the end winding, we have noticed that the experimental temperature curves trend of the end winding are close in trend to Al-Tayie temperature curves, this support the thermal model proposed in this study.

It can be seen from Figure 31, and Figure 32 , that the present study results were consistent with other studies conducted on induction motor. The differences in the values maybe attributed to the use of different power rate induction motors than present study.

9. CONCLUSION

This study concentrated on the thermal analysis of the induction motors, where a thermal model is built using the lumped parameter thermal method, this thermal model is used to determine the temperature of the induction motor at different operating conditions (rated load and different values of applied torque at different values of stator frequency). The thermal model is used to give us a clear picture about the temperature distribution inside the induction motor, to give a precaution about any problems occur during the operating conditions, like the induction motor insulation, because If the internal temperature of the induction motor exceeded the motor's insulation thermal class, the motor's life would be reduced, a 10-deg C increase in motor operating temperature actually decreases the motor's useful service life by half.

The heat losses can be predicted by analytical solution, where the stator copper losses has a significant part of the

total losses , hence they depend on the stator current , which has the main effect in heating the induction motor. The stator current can be increased by increasing the value of the applied torque or by running the induction motor at a small values of the stator frequency at constant applied torque, when the induction motor is running at small rotational speeds, the values of heat transfer coefficients outside and inside the induction motor are decreased, and this effects on the cooling efficiency.

The temperature of each element in the induction motor at rated conditions is obtained, and we found out the temperature of each element at different values of applied torque, then we saw how these temperatures were changed by reducing the stator frequency at a constant load, then we noted that the limiting thermal factor is the copper winding temperature, which can damage the plastic slot liners.

The experimental results presented for the stator core, right end winding, left end winding, round frame, left side frame, and right side frame, and showed that the proposed thermal model of induction motor is capable of calculating the temperatures in the induction motor elements with good accuracy at different operating conditions by a percentage error from 3% to 5%. The errors between the measured and calculated temperatures are probably from thermocouples which measure only the outside temperature of the stator windings, stator core, and the frame. Also probable error may be from the calculation of the model's thermal resistances and heat capacitances, which depend on the material properties of the induction motor and geometrical dimensions. Also there are errors may be due to omitting the radiation heat transfer from the calculation or due to ignoring the friction losses in the bearing. However, these errors are within acceptable limit for practical purposes, where more than one thermo- couple were used to represent a particular point in the test machine (for instance، end-winding, stator core, the frame, etc) to reduce the errors.
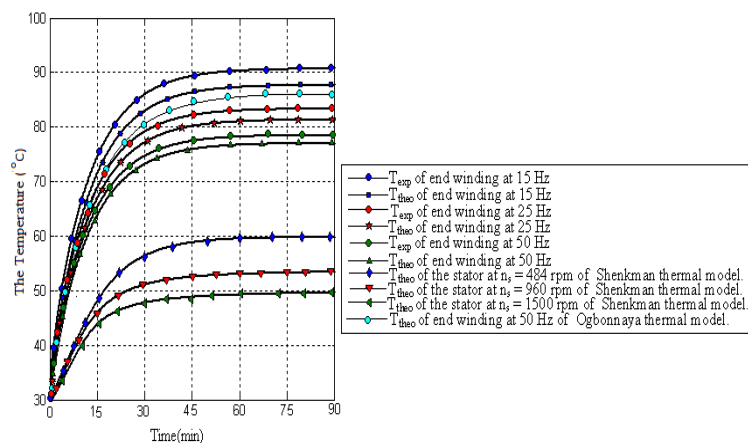

Figure 31- The comparison between the present thermal model and different thermal models for other researchers at rated load
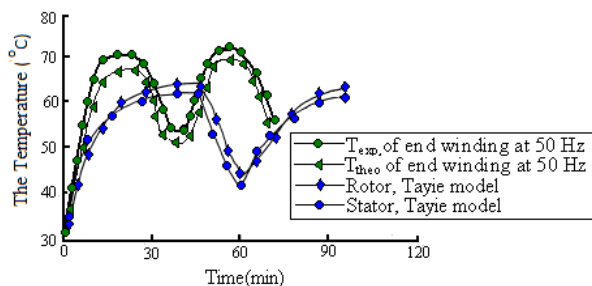
Figure 32- The comparison between the present thermal model and Tayie thermal model at different torques

REFERANCES

[1] www.lut.fi/fi/technology/electrical_engineering/research/electricaldrives/publications/Documents/Väitöskirjat/Puranen_doctoral.pdf

[2] Bimal K.Bose, Modern power electronics and AC drives, Prentice Hall PTR 2002

[3] Charles l.Hubert, Electric Machines – theory, operation, applications, adjustment, and control, PEARSON 2002

[4] Mellor et al ," Lumped parameter thermal model for electrical machines of TEFC design ", IEE Proceedings-B,Vol.138,No.5, April 1991

[5] Yangsoo Lee, "thermal analysis of induction motor with forced cooling channels", IEEE, magnetics, Vol.36, NO4, July 2000.

[6] Mario J. Durán, "Lumped parameter thermal model for induction motors", IEEE, energy conversion Vol.15, June 2004.

[7] Sreehivasan and Sengupta, "thermal design of totally enclosed fan cooled induction motors", IEEE winter PES, NY 1977.

[8] Dokopoulos and Xypteras, "analysis of transient temperature distribution in a rotating machine", electrical machines Sept 1982.

[9] Stephen J.Chapman, Electric machinery fundamentals, McGraw Hill 2005.

[10] Ogbonnaya I. Okoro, "Steady and Transient States Thermal Analysis of a 7.5-kw Squirrel-Cage Induction Machine at Rated-Load Operation", IEEE, energy conversion, vol. 20, no. 4, December 2005.

[11] www.ece.msstate.edu/~donohoe/ece3414induction_machines_II.pdf

[12] www.electro-tech-online.com/general-electronics-chat/7587-test-inductor-motor-no-   load-blocked-rotor-test.html35 - k

[13] Rosenberry, G.M.Jr.," the transient stalled temperature rise of the cast aluminum squirrel rotors for induction motors", AIEE, vol, PAS-74, Oct 1955

[14] Williamson and Walker, "calculation of stall bar temperature rise", 5th Int. Conf. on electrical machines and drives, Sept 1991.

[15] Frank P.Incropera, David P.DeWitt, Fundamentals of heat and mass transfer, John Wiley and Sons 2002.

[16] Ying Huai, Roderick V. N. Melnik, "Computational analysis of temperature rise phenomena in electric induction motors", Science Direct, Applied Thermal Engineering, Volume 23, Issue 7, May 2003, Pages 779-795.

[17] Staton D.A., Cavagnino A., "Convection Heat Transfer and Flow Calculations Suitable for Analytical Modeling of Electric Machines ", IEEE Industrial Electronics , Nov. 2006.

[18] Taylor, G.I.,"Distribution of Velocity and Temperature between Concentric Cylinders", Proc Roy Soc, 1935,   159, PtA, pp 546-578

[19] Gazley, C.: 'Heat Transfer Characteristics of rotating   and axial flow between concentric cylinders', ASME, Jan 1958, pp.79-89.

[20] Powek Witzak, "the transient heat flow in stator of the high voltage induction motor", evolution and modern aspects of induction machines, July 1986.

[21] Gnffith and McCoy," induction motor squirrel cage rotor winding thermal analysis", IEEE, Vol.-EC-1, N-3, sept 1986.

[22] Yuangjiang Liu," 3D thermal stress analysis of the rotor of an induction motor", IEEE, magnetics, Vol. 36, NO4, July 2000

[23] Siyambalapitiya et a1," transient thermal characteristics of induction motor rotor cage ", IEEE, V-3, N-4, Dec 1988.

[24] Rajagopal et al," Axi-symetric steady state thermal analysis of totally enclosed fan cooled induction motors using FEM", CAD/CAM ,Aug 1994.

[25] J. K. Al-Tayie and P. P. Acarnley, "Estimation of speed, stator   temperature and rotor temperature in cage induction motor drive using the extended Kalman filter algorithm," IEE Proc. - Electr. Power Appl., vol. 144, pp. 13-20, 1997.

[26] Shenkman, " Thermal behaviour of induction motors under different speeds" IEE Proc., Electr. Power Appl, Volume 152,September 2005.